Validation of Microfocus Computed Tomography in the Evaluation of Bone Implant Specimens

Nele Stoppie, DDS;* Jan-Paul van der Waerden, BSc;† John A. Jansen, DDS, PhD;†
Joke Duyck, DDS, PhD;* Martine Wevers, ir, PhD;‡ Ignace E. Naert, DDS, PhD*

ABSTRACT

Background: Microfocus computed tomography (μCT) is an emerging technique owing to its speed, full three-dimensional information, and nondestructive properties.

Purpose: The aim of this study was to explore the efficacy of a μCT system (Philips HOMX 161™, Philips Medical Systems GmbH, Hamburg, Germany) for visualization of the bone structure around screw-type titanium implants by comparing μCT images with their histologic homologues.

Materials and Methods: Eight screw-type titanium implants were placed in the femoral condyles of two goats. After the excised implant-bone specimens were embedded in resin, three-dimensional μCT of the excised implant and bone specimens was performed. Histologic sections were subsequently made. A total of 150 histologic sections were matched with μCT images.

Results: Bone trabeculae were clearly visible on the μCT scans. However, bone close to the implant or present in the apical surface features of the implant could not be detected. The overall matching between μCT scans (slices) and the histologic sections was 89%.

Conclusion: Investigation of trabecular bone around titanium implants by μCT can be considered highly reliable for determining trabecular bone parameters, with the exception of measuring direct bone-to-implant contact.

KEY WORDS: histology, implant, microfocus computed tomography, trabecular bone

The microfocus computed tomography (μCT) technique was first described by Feldkamp and colleagues.[1] It is based on the same principles as those of medical computed tomography (CT), but its resolution is 100-fold enhanced. The advantages of the μCT technique as compared with other visualization techniques are its nondestructive character, two-dimensional reconstruction in arbitrary planes, full three-dimensional information, and a wide field of applications on different materials.

*Department of Prosthetic Dentistry/BIOMAT Research Group, School of Dentistry, Oral Pathology and Maxillofacial Surgery, Catholic University Leuven, Leuven, Belgium; †Department of Biomaterials, University Medical Center, Nijmegen, the Netherlands; ‡Department of Metallurgy and Materials Engineering, Catholic University Leuven, Leuven, Belgium

Reprint requests: Ignace Naert, Department of Prosthetic Dentistry/BIOMAT Research Group, Kapucijnenvoer 33, 3000 Leuven, Belgium; e-mail: ignace.naert@med.kuleuven.ac.be

Its application in the medical[2–4] and dental[5–9] fields is nowadays widespread. Because two-dimensional histologic data provide only limited information on three-dimensional structures, the complex architecture of trabecular bone specimens was one of the first objects of interest to be visualized by μCT.[10,11] This makes μCT attractive also for the investigation of bone response to oral implants. However, scanning a trabecular bone specimen including a titanium implant poses a challenge owing to the differing attenuation characteristics of bone and titanium. Van Oosterwyck and colleagues[8] were among the first who succeeded in visualizing individual bone trabeculae around a titanium implant by means of μCT; however, no quantitative analysis was performed. A few other studies[10,12,13] had already focused on the comparison of bone parameters between histologic images and μCT images. It is a misunderstanding that a good correlation between parameters should necessarily mean identical images. In Figure 1 the area and perimeter of the features in both

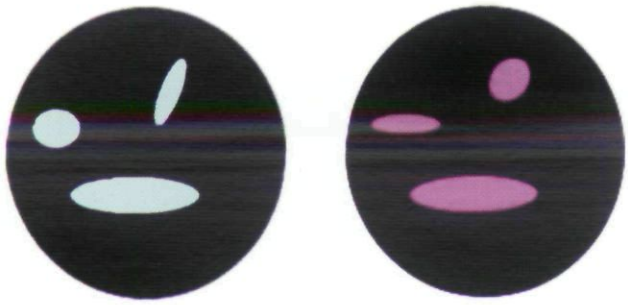

Figure 1 Representation of two different images with equal areas and perimeters of the features inside.

images are equal although they are not identical. Consequently the aim of this study was to validate the μCT technique for detecting bone morphometric parameters by comparing the spatial distribution of bone between histologic sections and its μCT homologues. This was done by matching both images, section per section, for the whole bone-implant specimen.

MATERIALS AND METHODS

Two healthy adult female Saanen goats weighing about 60 kg were used in this experiment. A longitudinal incision was made on the medial surface of the left and right femoral condyles. This model was chosen to fully seat the implants into trabecular bone. After exposure of the medial condyle, two 1.6 mm pilot holes were made (the distance between the holes was at least 1 cm). The holes were gradually widened with larger drills to the final diameter of the implant (3.5 mm). The 3.5 mm–diameter 13 mm–long screw-shaped titanium implants (Astra Tech, Mölndal, Sweden) were inserted by hand. Cover screws were placed on top of the implants. In this way each condyle received two implants. The installation was performed while the goats were under general anesthesia. After 6 weeks the goats were sacrificed with an overdose of pentobarbital. The femoral condyles with the eight implants were excised and fixed immediately in 4% buffered formaldehyde solution. Via standard histologic technique, the tissue blocks were dehydrated by series of alcohol. Before being embedded, the specimens were trimmed to their final cylindrical shape (8 mm in diameter and 13 mm in length). To ensure the central position of the implant in the bone specimen, the cover screw was removed and a pin was tightened on the implant before the size of the samples was reduced with a trephine drill. A total of eight specimens were mounted on a holder that served as a reference plane and were embedded in resin.

This study was approved by the Animal Ethical Committee of the Catholic University, Leuven. National guidelines for the care and use of laboratory animals were observed.

Microfocus CT Scanner

The Philips HOMX 161™ microfocus radiography system (Philips Medical Systems GmbH, Hamburg, Germany) was upgraded with Tomohawk® CT software and hardware (AEA Technology, Oxon, UK). The device was equipped with a microfocus x-ray tube with a focal spot of 5 μm, producing a cone beam detected by a TH 9438HX image intensifier (Thales Electron Devices, Vélizy, France). The resulting light was detected by a 1,024 × 1,024 pixel charge-coupled-device (CCD) camera (Adimec, Eindhoven, the Netherlands), which gave the digital signal to a frame grabber card (Imaging Technologies Inc, Atlanta, GA) connected to a personal computer (Dell™, Dell Inc., Round Rock, TX, USA) using a dual Pentium® III 933 MHz microprocessor (Intel Corporation, Santa Clara, CA, USA) and Windows® NT operating system software (Microsoft Corporation, Redmond, WA, USA) (Figure 2). The resulting images are 12-bit grayscale images at a resolution of 1,024 × 1,024 pixels. The rotational and axial shifts of the turntable were effectuated with a Servostep 1700 motor (Naples Coombe, Berkshire, UK). An optimized three-dimensional cone beam reconstruction algorithm (based on that described by Feldkamp and colleagues)[14] with a Bracewell and Riddle inverse filter was used. Two specimens were used as pilot cases to set up the protocol for μCT. The specimen on the holder was placed on the turntable, and a three-dimensional scan was taken at 100 kV, 0.13 mA, and a rotation step of 0.5° for a rotation angle of 186°. A 2 mm–thick aluminum filter was placed between detector and specimen to reduce artifacts from the titanium. A full three-dimensional image of the whole implant with surrounding trabecular bone was obtained with a cubic voxel size of 24 μm at resolution 512 of reconstruction, resulting in about 500 two-dimensional images per specimen (Figures 3A and 4A).

The position of every μCT cross section relative to the middle of the bone-implant specimen was defined by means of the known voxel size.

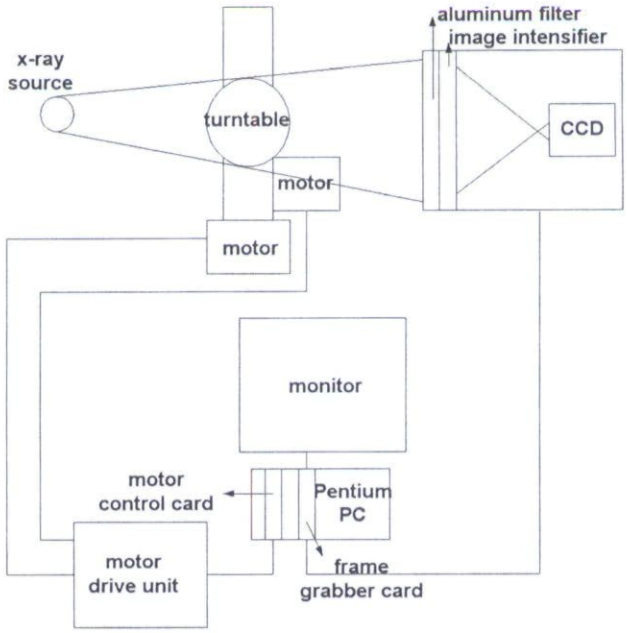

Figure 2 Overview of the Philips HOMX 161 microfocus radiography system upgraded with the Tomohawk computed tomography software. The sample is positioned on the turntable. (CCD = charge-coupled device; PC = personal computer)

Histologic Sections

The same two specimens mentioned above were used to define the histologic protocol. The sample holder was used to mount the specimen in a modified inner-circular-saw microtome,[15] and nondecalcified sections of 30 μm were made parallel to the reference plane. Only optimal sections were retained (66%) and stained with methylene blue and basic fuchsin for evaluation with light microscopy (see Figures 3B and 4B). The exact amount of material lost during sectioning was measured each time by an external micrometer with a precision of 3.0 μm (Sony U60AF™, Schut, Groningen, the Netherlands), and the output value of the micrometer was used to define the corresponding μCT slices.

Matching of μCT Slices and Histologic Sections

To identify bone and nonbone structures, both types of images were processed with Q-Win® software (Leica Microsystems, Rijswijk, the Netherlands). For the μCT slices of each specimen, the optimal threshold value was identified as the steepest gradient of gray levels.[6,16] Because the two pilot specimens were excluded for the final analysis, the average optimal threshold was calculated from the six remaining specimens (25% of the maximum gray level of bone) and was applied to the specimens, resulting in six defined thresholds. With

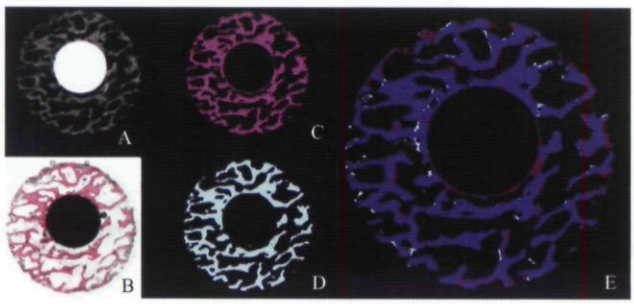

Figure 3 Images made at the midcross section of the implant body. The μCT slice (A) is segmented for bone, resulting in a red binary image (C). The corresponding histologic section (B) is segmented for bone, resulting in a blue binary image (D). The matching image (E) of the binary images presents three colors: purple (where both blue and red are present), nonfitting blue, and nonfitting red.

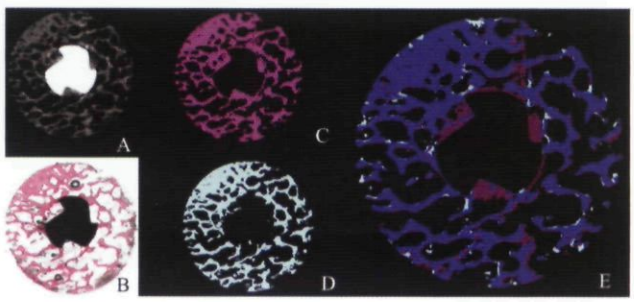

Figure 4 Images of the same parameters shown in Figure 3, focusing on the apical part of the implant.

the Q-Win software program, all gray values above this threshold per specimen were given a specified color. To make a clear distinction, red was chosen for the μCT slices and blue was chosen for the histologic sections. The segmenting for bone was run automatically and resulted in red binary images for the μCT slices (see Figures 3C and 4C). The threshold defining bone for the histologic sections was set manually for each individual section, resulting in blue binary images (see Figures 3D and 4D). These binary images were matched by an advanced graphic package for Windows (Xara X®, Xara Ltd, Hempstead, UK), and the matched area was colored purple (Figure 5). In the resulting image three colors were present: red, blue, and purple (see Figures 3E, 4E, and 5). Detection of these three colors was performed, and the area was calculated. The purple area represented the matching zone between μCT slice and histologic section. The blue area corresponded to the nonfitting remainder of the histologic image, and the red area corresponded to the nonfitting remainder of the μCT image. The histologic sections served as a reference, and the bone was defined as the sum of purple and blue areas in the matched image (see Figures 3E and 4E). The bone in the μCT slices was defined as the sum of purple and red areas in the matched image (see Figures 3E and 4E). Bone area measurements for the μCT slices and histologic sections were expressed as percentages. Three other parameters were chosen to compare the μCT slices with the histologic sections: purple/histologic section, red/μCT slice, and blue/histologic section.

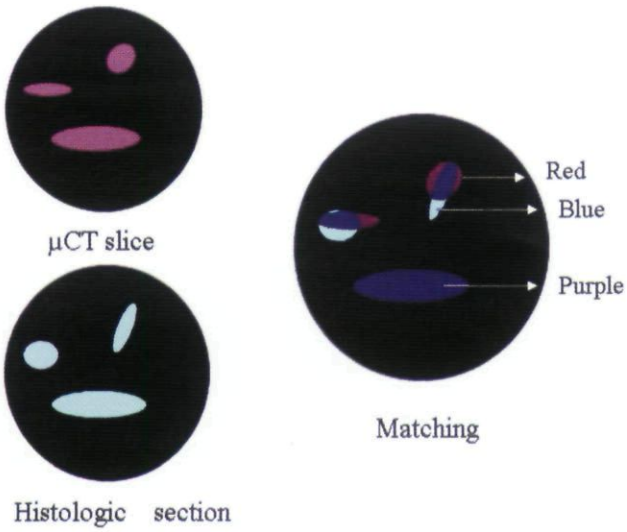

Figure 5 Illustration of the principle of matching the microfocus computed tomography (μCT) slice (*red*) with the corresponding histologic section (*blue*).

Statistical Analysis

Means and 95% confidence intervals for the bone area measurements (histology and μCT) and the three above-mentioned parameters (purple/histologic section, red/μCT slice, and blue/histologic section) were calculated. A distinction was made between calculations per specimen and overall calculations. Overall mean and confidence interval calculations were made by means of a linear mixed model, with goat and specimen as random effects. This was done to take into account the correlation induced by the clustered structure of the data. Indeed the observations were not independent since they were clustered within a specimen. Moreover the specimens were clustered within a specific goat.

For each specimen separately, bone measurements between the two methods were compared by using *t*-distribution-based confidence intervals and paired *t*-tests. Spearman's correlation was used to explore (1) the relations between position within the specimen to its middle and the three aforementioned parameters (purple/histologic section, red/μCT slice, and blue/histologic section), (2) the relation between the bone measurements obtained with the two methods, and (3) the evolution of the latter relation as a function of its position relative to the middle of the specimen.

All analyses were performed with SAS® version 8.2 statistical software (SAS Institute Inc., Cary, NC, USA). The linear mixed model was fitted by the PROC MIXED procedure.

RESULTS

Owing to positioning errors during the preparation for histologic sectioning, the two pilot specimens were excluded in the final analysis. For the remaining six bone-implant specimens, 150 histologic sections were selected together with the 150 corresponding μCT slices. The bone trabeculae were clearly visible on the μCT slices. However, bone close to the implant or present in the apical surface features of the implant could not be detected. A thin layer of noise around the implant (60 μm) was present along the whole implant surface (see Figure 3A). At the implant's apical end, noise was filling the implant threads (see Figure 4A). Attempts to filter this noise resulted in loss of the

TABLE 1 Means and 95% Confidence Limits of Bone Area Measurements of Histologic Sections and Microfocus Computed Tomography Slices, per Specimen

	Histologic Sections		μCT Slices	
Specimen No.	Mean (%)	95% CLs	Mean (%)	95% CLs
1	27.15	25.35, 28.95	31.92	30.31, 33.52
2	28.48	27.53, 29.44	37.68	36.32, 39.04
3	34.21	31.41, 37.02	41.18	38.57, 43.80
4	28.90	25.71, 32.09	40.30	36.89, 43.71
5	33.30	30.89, 35.72	38.04	35.65, 40.43
6	29.81	26.00, 33.62	39.77	36.10, 43.44

μCT = microfocus computed tomography; CLs = confidence limits.

finest trabeculae. Considering the whole data set of 150 images, the overall matching between μCT slices and histologic sections was 89.23% (95% confidence interval [CI], 87.40–91.05). The mean remaining red area of the μCT slice was 29.3% (95% CI, 24.66–33.94), and the mean remaining blue area of the histologic section was 10.77% (95% CI, 8.95–12.6).

The means and the 95% confidence limits of the bone area measurements per specimen for the histologic sections and the μCT slices are listed in Table 1. The overall mean bone area was 29.82% for the histologic sections and 37.45% for the μCT slices (linear mixed model). A significant difference was found between the bone area measurements of the histologic sections and those of the μCT slices at the overall level ($p < .0001$, linear mixed model) and at the specimen level ($p < .0001$, paired t-tests). On average the bone area measurement made with the μCT technique was 7.95% (standard error [SE], 0.74) higher than the measurement made on the histologic sections. Spearman's correlations between the bone area measurements of both techniques were calculated per specimen (Table 2). The overall Spearman's correlation was 0.86 (linear mixed model).

The μCT slices were well reconstructed not only in the middle but also at the top and bottom parts of the field of view (Figure 6). No statistically significant correlation between location of the μCT slice within the specimen and one of the parameters (purple/histologic section, red/μCT slice, and blue/histologic section) could be found. The same conclusion was drawn for the evolution of the relation between μCT-based and histology-based measurements in function of the position (Figure 7). There is no indication that this relation varied according to the position of the slice within the specimen.

TABLE 2 Spearman's Correlations Between Bone Area Measurements of Histologic Sections and Microfocus Computed Tomography, per Specimen

Specimen No.	Spearman's Correlation
1	0.84
2	0.58
3	0.95
4	0.95
5	0.93
6	0.95

DISCUSSION

Histologic sectioning was chosen as the "gold standard" because of (1) better resolution (to 1 μm) when compared with the μCT technique, (2) the possibility for digitization of the whole histologic section without division of the image, and (3) the ease of color detection for the segmenting of bone. The total number of histologic sections for the plastic-embedded

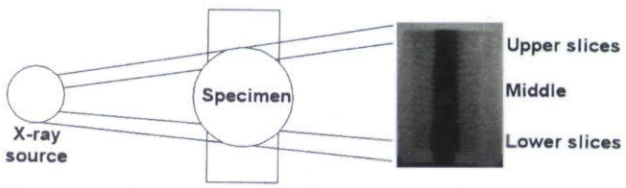

Figure 6 Radiographic view of the specimen of trabecular bone with implant, with diagram showing the division of the location of the microfocus computed tomography slices into upper, middle, and lower parts.

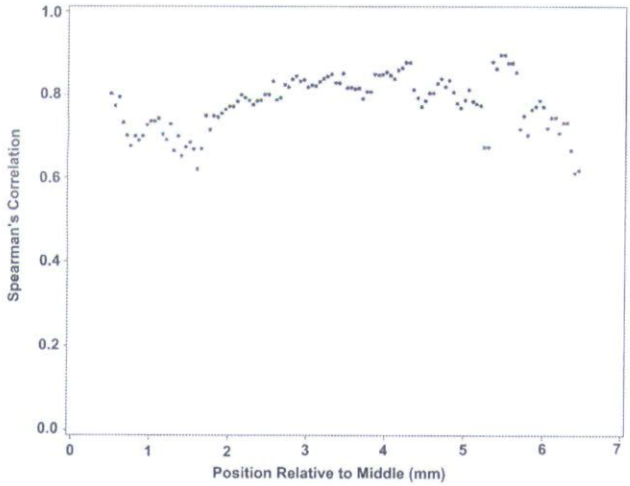

Figure 7 Graph showing the relation between the slice position within the specimen (in millimeters) and Spearman's correlation, between bone area measurements made with microfocus computed tomography and those made with histologic sections.

specimens was less than the number of μCT slices. Because of the thickness (300 μm) and the vibration of the sawing blade, a mean distance of 380 μm existed between the separate histologic sections whereas the mean separation distance for the μCT slices was 24 μm.

The titanium caused a blurred border of 60 μm along the whole implant surface. At the apical end of the implant, the scatter of titanium and the geometry of the implant were responsible for the filling of the threads with noise. Metal artifacts are due to a combination of beam hardening, scatter, nonlinear partial volume effect, and noise.[17] An aluminum filter was placed between detector and specimen to reduce artifacts from the titanium. This filter reduced secondary radiation and suppressed (but not completely) the streak artifacts. As a consequence bone contact could not be accurately measured around full metallic implants. Bone trabecular parameters can be measured well at a distance of 60 μm and out of the implant threads at the apical end. Polyethylene implants with an ultrathin titanium coating are an option for measuring bone-implant contact (data are to be published).

The mean matching area was 89% for the whole data set. One may wonder why the remaining 11% did not match between the μCT slice and the histologic section. This mismatch was expressed in function of the origin as the mean red area for the μCT slice and the mean blue area for the histologic section. The volume remaining red (29%) in the μCT slice was more important than the volume remaining blue (10%) in the histologic section. Several reasons for this may be considered. First, noise was present in the μCT images as a fine layer around the implant's body and in the surface features at the apical end of the implant. Second, the discrepancy of section thickness has to be considered; our histologic sections were about 30 μm thick whereas the μCT slice was 24 μm thick. Third, there were small deviations between the direction of the x-rays and the cutting plane of the circular saw although the specimens were mounted on a specially designed holder for transfer from the μCT device to the circular saw. The beam of x-rays was a cone beam, which implies that in the middle of the field of view, the x-rays were perpendicular to the specimen (see Figure 6). Away from this middle the x-rays crossed the specimen at an angle other than 90°. Therefore a correction was made in the reconstruction algorithm, resulting in an optimized three-dimensional cone beam reconstruction as described by Feldkamp and colleagues.[14] The fact that no relation could be found with the position within the specimen indirectly proved that this correction worked properly. Nevertheless small differences cannot be fully excluded. Finally, the choice of the threshold influenced the detected bone volume. In the present study an analysis of changes in the μCT threshold revealed a 4% change in bone volume fraction with a 5% variation of threshold. These results lie in between those of Rüegsegger and colleagues[11] and those of Giesen and van Eijden.[6] The former found a change in bone volume fraction of 5% with a 10% change of threshold whereas the latter obtained a 7.9% bone volume fraction change with a 5% change of threshold. Ding and colleagues[16] compared the bone volume fractions determined with the adaptive threshold procedure and with Archimedes' principle. According to their definition, our six specimens belong to the high-density specimens (volume fraction, > 30%), and for this subgroup the overestimation of volume fraction was 7.2% by the adaptive threshold procedure. This overestimation can partially explain the remaining red in the μCT slice as well.

The bone area measurements confirmed the findings from matching μCT and histology. The overall mean bone areas were 29.82% for the histologic sections and 37.45% for the μCT slices. The bone area as measured with the μCT technique was 7.95% (SE, 0.74) higher than that measured on histologic sections. This corresponded with the more important volume that

remained red (29%) in the μCT slice than the volume that remained blue (10%) in the histologic section.

Currently one report validates μCT and histologic data on bone around metallic implants.[18] Histology- and μCT-based measurements of bone volume, trabecular thickness, trabecular separation, and bone connectivity were compared. Investigators found that the standard histomorphometric technique gave values that were slightly higher than the values obtained with μCT. However, care should be taken when comparing these studies. This article was based on the mean values of 150 images of 6 specimens. In the study by Rebaudi and colleagues,[18] the comparisons were based on the mean values of 400 μCT slices and 3 histologic sections for only one specimen. The bone apposition was defined at a distance of 45 μm of the implant. This finding corresponds to our finding that boundary blurring was present and that at the moment no bone contact could be measured around metallic implants. In our study a 60 μm–wide layer was found, compared to the 45 μm boundary described by Rebaudi and colleagues.[18] This could be explained by the difference of thickness between both titanium implants (2.0 mm and 3.5 mm). The thicker the titanium implant, the larger the influence on the quality of the μCT image.

Considering the bone area measurements, our findings corroborate those of studies that compared μCT and histologic studies of just trabecular bone specimens by means of bone parameters. The overall Spearman's correlation was 0.86. When looking at the specimen level (see Table 2), one can conclude that specimen number 2 caused a decrease in the overall result because of its lower correlation coefficient (0.58). This meant that no constant trend could be detected between the two measurements. However, the comparison of the mean bone area values for histology (28.48%) and μCT (37.68%) followed the observation of higher bone area values for the μCT technique. For 36 trabecular human transiliac bone specimens, Müller and colleagues[13] compared bone volume density and bone surface density, trabecular thickness, and trabecular separation as measured by both conventional histomorphometry and μCT. Their results showed highly significant ($p < .0001$) correlations for bone volume density ($r = 0.93$) and bone surface density ($r = 0.91$), trabecular thickness ($r = 0.84$), and trabecular separation ($r = 0.91$).

With 50 human iliac bone samples, Ito and colleagues[12] compared conventional histomorphometry with μCT in terms of bone volume, trabecular number, trabecular thickness, and trabecular separation. Both two- and three-dimensionally based parameters from μCT correlated significantly with the parameters from conventional histomorphometry ($r = 0.63$–0.86 in two-dimensional analysis, and $r = 0.60$–0.77 in three-dimensional analysis).

CONCLUSION

Microfocus computed tomography can be considered a highly reliable tool for determining trabecular bone parameters, except that of bone contact around metallic implants. Because of its nondestructive character, speed of scanning procedure, and full three-dimensional information, this technique supersedes histologic sectioning.

ACKNOWLEDGMENTS

This study was supported by the Fund for Scientific Research, Flanders (No. 101/8 and 1.5.118.02, Belgium).

Annelies Ghesquiere and Steffen Fieuws (Biostatistical Center, School of Public Health, Leuven, Belgium) are acknowledged for performing statistical analysis of the data. Astra Tech AB (Mölndal, Sweden) is acknowledged for providing the implants.

REFERENCES

1. Feldkamp LA, Goldstein SA, Parfitt AM, Jesion G, Kleerekoper M. The direct examination of three-dimensional bone architectures in vitro by computed tomography. J Bone Mineral Res 1989; 4:3–11.
2. Kapadia RD, Stroup GB, Badger AM, et al. Applications of micro-CT and MR microscopy to study pre-clinical models of osteoporosis and osteoarthritis. Technol Health Care 1998; 6:361–372.
3. Verna C, Bosch C, Dalstra M, Wikesjö UME, Trombelli L. Healing patterns in calvarial bone defects following guided bone regeneration in rats. A micro-CT scan analysis. J Clin Periodontol 2002; 29:865–870.
4. Patel V, Issever AS, Burghardt A, Laib A, Ries M, Majumdar S. MicroCT evaluation of normal and osteoarthritic bone structure in human knee specimens. J Orthop Res 2003; 21:6–13.
5. Balto K, Müller R, Carrington DC, Dobeck J, Stashenko P. Quantification of periapical bone destruction in mice by micro-computed tomography. J Dent Res 2000; 79:35–40.
6. Giesen EB, van Eijden TM. The three-dimensional cancellous

bone architecture of the human mandibular condyle. J Dent Res 2000; 79:957–963.

7. Sennerby L, Wennerberg A, Pasop F. A new microtomographic technique for non-invasive evaluation of the bone structure around implants. Clin Oral Implants Res 2001; 12:91–94.
8. Van Oosterwyck H, Vander Sloten J, Van der Perre G, Jansen J, Wevers M, Naert I. The use of microfocus computerized tomography (micro-CT) as a new technique to characterize bone tissue around oral implants. J Oral Implantol 2000; 26:5–12.
9. Bergmans L, Van Cleynenbreugel J, Wevers M, Lambrechts P. A methodology for quantitative evaluation of root canal instrumentation using microcomputed tomography. Int Endod J 2001; 34:390–398.
10. Kuhn JL, Goldstein SA, Feldkamp LA, Goulet RW, Jesion G. Evaluation of a microcomputed tomography system to study trabecular bone structure. J Orthop Res 1990; 8:833–842.
11. Rüegsegger P, Koller B, Müller R. A microtomographic system for the nondestructive evaluation of bone architecture. Calcif Tissue Int 1996; 58:24–29.
12. Ito M, Nakamura T, Matsumoto T, Tsurusaki K, Hayashi K. Analysis of trabecular microarchitecture of human iliac bone using microcomputed tomography in patients with hip arthrosis with or without vertebral fracture. Bone 1998; 23:163–169.
13. Müller R, Van Campenhout H, Van Damme B, et al. Morphometric analysis of human bone biopsies: a quantitative structural comparison of histological sections and microcomputed tomography. Bone 1998; 23:59–66.
14. Feldkamp LA, Davis LC, Kress JW. Practical cone beam algorithm. J Opt Soc Am 1984; 1:612–619.
15. van der Lubbe HB, Klein CP, de Groot K. A simple method for preparing thin (10 μm) histological sections of undecalcified plastic embedded bone with implants. Stain Technol 1988; 63:171–176.
16. Ding M, Odgaard A, Hvid D. Accuracy of cancellous bone volume fraction measured by micro-CT scanning. J Biomech 1999; 32:323–326.
17. Suetens P. Fundamentals of medical imaging. Cambridge, UK: Cambridge University Press; 2002. p. 85–87.
18. Rebaudi A, Koller B, Laib A, Trisi P. Microcomputed tomographic analysis of the peri-implant bone. Int J Periodontics Restorative Dent 2004; 24:316–325.